

## Configuration mixing and $K$ -forbidden $E2$ decays

P. M. Walker<sup>1</sup>\* and P. D. Stevenson<sup>1</sup>

*Department of Physics, University of Surrey, Guildford, GU2 7XH, United Kingdom*



(Received 8 April 2021; accepted 26 May 2021; published 7 June 2021)

Hindrance factors for  $K$ -forbidden  $E2$  decays from multiquasiparticle isomers are analyzed in relation to mixing matrix elements that are often associated with chance near degeneracies, and a functional relationship is established. Focusing on effective matrix elements for  $\Delta K = 6$  decays from three-quasiparticle isomers, significant configuration dependence is demonstrated.

DOI: [10.1103/PhysRevC.103.064305](https://doi.org/10.1103/PhysRevC.103.064305)

### I. INTRODUCTION

With half-lives ranging from nanoseconds to years, and excitation energies up to almost 15 MeV, nuclear isomers play an important role in nuclear structure, nuclear astrophysics, physics at the atomic/nuclear interface, and applications [1–6]. In deformed nuclei, a key determinant of electromagnetic transition rates is the  $K$  quantum number, i.e., the projection of the angular momentum on the nuclear symmetry axis. However, despite extensive studies [5,7], the understanding of transition rates remains rudimentary for transitions that involve significant changes in the  $K$  value.

Deformed nuclei have rotational bands based on different quasiparticle ( $qp$ ) configurations. It is usually assumed that, to a good approximation, the  $K$  value is equal to the spin of the bandhead, providing the bandhead is well defined experimentally, such as when it is isomeric. The decays of isomeric bandheads are often associated with so-called  $K$ -forbidden transitions, which arise when the change in the  $K$  value,  $\Delta K$ , exceeds the angular momentum,  $\lambda$ , carried by the decay radiation [5,7]. The degree of forbiddenness is defined as  $\nu = \Delta K - \lambda$ . Due to  $K$  mixing, such transitions are not strictly forbidden, and  $K$ -isomer half-lives are sensitive to the amount of mixing, both in the isomers themselves and in the states to which they decay.

Although it is tempting to say that  $K$  mixing destroys the goodness of the  $K$  quantum number, it is notable that  $K$  isomers typically have only small admixtures of states with different  $K$  values. In such circumstances, it is reasonable to specify and discuss the dominant  $K$  value that characterizes any given  $K$  isomer.

Numerous attempts have been made to pin down the important degrees of freedom that influence  $K$ -isomer half-lives, beyond the relatively simple dependence on transition energy, multipole character, and degree of forbiddenness [5,7]. These latter aspects can be accounted for by calculating the Weisskopf hindrance factor,  $F_W = (T_{1/2}^\gamma/T_{1/2}^W)$ , where  $T_{1/2}^\gamma$  is the partial  $\gamma$ -ray half-life and  $T_{1/2}^W$  is the corresponding

Weisskopf value, and then obtaining the reduced hindrance,  $f_\nu = (F_W)^{1/\nu}$ . Following this procedure, any reduced-hindrance variations should be due to the nuclear structure. Indeed, for different isomers, there can be large variations in reduced hindrance, both within a given nuclide and between different nuclides. Possible physical explanations for the  $f_\nu$  variations include rotational (Coriolis)  $K$  mixing, dynamic and static axially asymmetric ( $\gamma$ ) distortions, statistical  $K$  mixing due to level-density effects, and chance near degeneracies with states of the same spin and parity [5,7]. The reduced hindrance may also depend on the specific  $qp$  configurations involved [7,8]. Furthermore, reduced-hindrance correlations have been found with other variables [5,7], such as the product of the valence nucleon numbers,  $N_p N_n$  [9,10], and the isomer energy relative to that of a rigid rotor [10–12]. However, substantial deviations from simple correlations indicate the importance of multiple degrees of freedom.

The present work generalizes the analysis of chance near degeneracies, where a  $K$  isomer is close in energy to a state of the same spin and parity but with a lower  $K$  value. Two-state mixing [13] can then lead to enhanced  $E2$  decay from the isomer. The mixing matrix elements,  $V$ , are calculated and shown to be closely related to the Weisskopf hindrance factors through a simple formula. After allowing for near degeneracies, examination of  $E2$ ,  $\Delta K = 6$   $\gamma$ -ray transitions from 3- $qp$  isomers reveals a dependence on three factors: the isomer excitation energy relative to a rigid rotor, the 1- $qp$  configuration of the populated state (to which the isomer decays), and the 3- $qp$  configuration of the isomer itself.

### II. TWO-STATE MIXING

In the study of isomeric decays, a recurring scenario is when there is a near degeneracy between an isomer and a member of the rotational band to which it decays, as represented schematically in Fig. 1. While the decay  $E2$  transition changes the spin by  $2\hbar$ , the relevant near degeneracy, with energy difference  $\Delta E$ , is between states of equal spin and parity. A small mixing amplitude,  $\beta$ , of the rotational-band wave function into the isomeric state can account for the half-life of the isomer, on the basis that the mixing provides a collective

\*p.walker@surrey.ac.uk

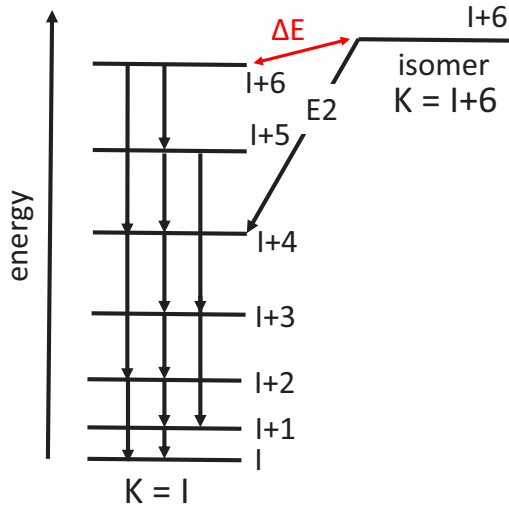


FIG. 1. Schematic level scheme illustrating a multi- $qp$  isomer, which decays by a  $\Delta K = 6$ ,  $E2$  transition into a rotational band.

component in the  $E2$  decay of the isomer. For example, in the decay of a 3- $qp$  isomer in  $^{171}\text{Tm}$  [14], the energy difference is  $\Delta E = 11$  keV. The isomer half-life of  $1.7 \mu\text{s}$  can be understood if there is a small collective admixture in its wave function, with a mixing matrix element of  $|V| = 12 \pm 2$  eV (only the modulus of  $V$  is obtained, not the sign). In this case, the collective admixture (amplitude squared) in the isomer is  $\beta^2 = 1.2 \times 10^{-6}$ . Mixing matrix elements of this kind have been compared, as a function of  $\Delta K$ , by Dracoulis *et al.* [15].

The analysis assumes the validity of the rotational model [16] for the in-band reduced transition probability,

$$B(E2) = \frac{5}{16\pi} e^2 Q_o^2 | \langle I_1 K 2 0 | I_2 K \rangle |^2, \quad (1)$$

and the rotor transition rate is

$$T(E2) = 1.22 \times 10^9 E_\gamma^5 B(E2) s^{-1} \quad (2)$$

with the transition energy,  $E_\gamma$ , in MeV, and  $B(E2)$  in units of  $e^2 \text{fm}^4$ . In the present work, the intrinsic quadrupole moment is evaluated [17] from

$$Q_o = \frac{3}{\sqrt{5\pi}} Z e r_o^2 A^{2/3} \beta_2 (1 + 0.36\beta_2) \quad (3)$$

with  $r_o \approx 1.2$  fm and the theoretical quadrupole deformation,  $\beta_2$ , is tabulated by Möller *et al.* [18]. Since the mixing strength is a small fraction of the energy gap,  $\Delta E$ , it is a good approximation to relate the mixing matrix element to the collective amplitude by [15]

$$|V| = \beta \times \Delta E. \quad (4)$$

Finally, the Weisskopf hindrance factor for an  $E2$  transition can be written [7]

$$F_W(E2) = 1.05 \times 10^8 T_{1/2}^\gamma E_\gamma^5 A^{4/3}, \quad (5)$$

and the relationship between the partial half-life of the  $E2$  transition from the isomer and the rotor  $E2$  transition rate is

$$T_{1/2}^\gamma(E2) = \frac{\ln 2}{\beta^2 T(E2)}. \quad (6)$$

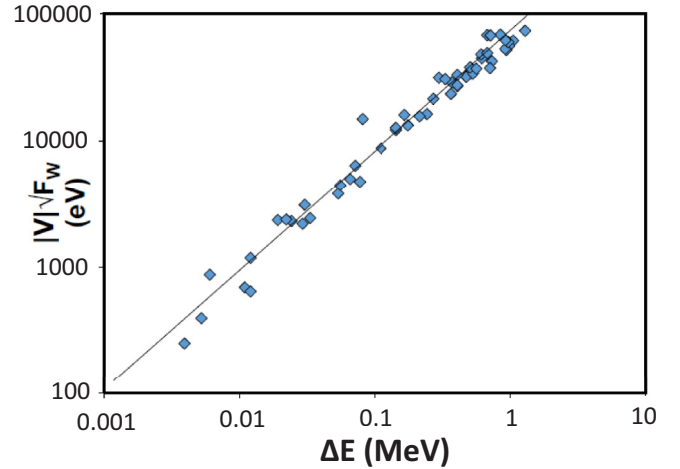


FIG. 2. Correlation plot for isomeric  $E2$  transitions, showing how the product of the mixing strength and the square root of the Weisskopf hindrance factor,  $|V|\sqrt{F_W}$ , varies with the energy separation,  $\Delta E$ , between the isomer and the state with the same spin and parity that is a member of the band to which the isomer decays. The straight line through the data is to guide the eye.

By simple rearrangement of these equations, the following dimensionless relationship is obtained:

$$\sqrt{F_W} = \frac{\Delta E}{|V|} \frac{0.71}{Z\beta_2(1 + 0.36\beta_2) | \langle I_1 K 2 0 | I_2 K \rangle |}. \quad (7)$$

In the present study, the multi- $qp$  isomers that will be analyzed in this way are limited to the  $Z \approx 70$  region, so that the  $Z$  variations have only a small effect, and so also the quadrupole deformations, with  $\beta_2 \approx 0.25$ , have little variation. More significant differences come from the Clebsch-Gordan coefficients, which vary by up to a factor three for examples considered.

In Fig. 2, the correlation of  $|V|\sqrt{F_W}$  with  $\Delta E$  is shown for a range of isomers in the  $Z \approx 70$  region, including all 18 cases with  $\Delta E < 0.1$  MeV [7,14,15,19–33]. In three of these,  $^{174}\text{Yb}$  [21],  $^{174}\text{Lu}$  [15], and  $^{181}\text{W}$  [27], it is necessary to extrapolate the populated band to reach the spin of the isomer, but the final values are not sensitive to this aspect. It can also be noted that the maximum deviation from the straight line through the data is for the  $\Delta E = 0.081$  MeV,  $K^\pi = 43/2^+$  isomer of  $^{177}\text{Ta}$  [19] with  $\Delta K = 4$ , which has the smallest Clebsch-Gordan coefficient.

A striking feature of Fig. 2 is that there is a single trajectory of the data, as specified by Eq. (7). Although the motivation for the derivation of the equation comes from the wish to analyze isomer decay rates associated with chance near degeneracies, there is no empirical indication of any constraint on the specification of “near”. The largest energy difference represented in the figure is  $\Delta E = 1.295$  MeV, associated with the  $E2$  decay of a  $K^\pi = 12^+$  isomer in  $^{164}\text{Er}$ , directly to the  $K^\pi = 0^+$  ground-state band [34]. It is possible, of course, to question the validity of the two-state mixing analysis for such widely spaced levels, but there is no sign of any systematic effect in Fig. 2. Indeed, according to Eq. (7) there cannot be large deviations, providing Eq. (4) remains valid, i.e., the

TABLE I. Three- $qp$  isomers with  $\Delta K = 6$ ,  $E2$  decays. The 3- $qp$  configurations and  $f_\nu$  values are from Kondev *et al.* [7] except where noted. Nuclide-specific references are also given. The 1- $qp$  configuration refers to the populated band.

Nuclide	$K^\pi$	$T_{1/2}$	$\Delta E^a$ (keV)	$f_\nu$	$ V $ (eV)	$E_K - E_R$ (keV)	3- $qp$ configuration	1- $qp$ configuration	Ref.
<sup>171</sup> Tm	19/2 <sup>+</sup>	1.7 $\mu$ s	-11	7.7	12	936	$\nu 5/2[512], \nu 7/2[633], \pi 7/2[523]$	$\pi 7/2[404]$	[14]
<sup>175</sup> Lu	19/2 <sup>+</sup>	960 $\mu$ s	368	85	3.2	681	$\nu 5/2[512], \nu 7/2[514], \pi 7/2[404]$	$\pi 7/2[404]$	[35]
<sup>171</sup> Hf	19/2 <sup>+</sup>	6.2 ns	929	13	355	907	$\nu 7/2[633], \pi 5/2[402], \pi 7/2[404]$	$\nu 7/2[633]$	[36]
<sup>175</sup> Hf	19/2 <sup>+</sup>	1.1 $\mu$ s	536	24	60	723	$\nu 7/2[633], \pi 5/2[402], \pi 7/2[404]$	$\nu 7/2[633]$	[37]
<sup>173</sup> Ta	21/2 <sup>-</sup>	148 ns	351	13	163	841	$\pi 5/2[402], \pi 7/2[404], \pi 9/2[514]$	$\pi 9/2[514]$	[38] <sup>b</sup>
<sup>175</sup> Ta	17/2 <sup>+</sup>	5.1 ns	501	7.6	569	977	$\pi 1/2[541], \pi 7/2[404], \pi 9/2[514]$	$\pi 9/2[514]$	[39]
<sup>175</sup> Ta	21/2 <sup>-</sup>	2.0 $\mu$ s	216	20	37	706	$\pi 5/2[402], \pi 7/2[404], \pi 9/2[514]$	$\pi 9/2[514]$	[39]
<sup>177</sup> Ta	17/2 <sup>+</sup>	5.5 ns	468	10	308	959	$\pi 1/2[541], \pi 7/2[404], \pi 9/2[514]$	$\pi 9/2[514]$	[19]
<sup>177</sup> Ta	21/2 <sup>-</sup>	5.3 $\mu$ s	53	23	7.3	511	$\pi 5/2[402], \pi 7/2[404], \pi 9/2[514]$	$\pi 9/2[514]$	[19]
<sup>179</sup> Ta	21/2 <sup>-</sup>	322 ns	-29	6.9	47	424	$\pi 5/2[402], \pi 7/2[404], \pi 9/2[514]$	$\pi 9/2[514]$	[23] <sup>c</sup>
<sup>181</sup> Ta	21/2 <sup>-</sup>	25 $\mu$ s	177	39	8.9	672	$\pi 5/2[402], \pi 7/2[404], \pi 9/2[514]$	$\pi 9/2[514]$	[35]
<sup>185</sup> Ta	21/2 <sup>-</sup>	12 ms	-272	71	4.3	490	$\nu 3/2[512], \nu 11/2[615], \pi 7/2[404]$	$\pi 9/2[514]$	[40] <sup>d</sup>
<sup>179</sup> W	21/2 <sup>+</sup>	390 ns	509	15	170	804	$\nu 5/2[512], \nu 7/2[514], \nu 9/2[624]$	$\nu 9/2[624]$	[26]
<sup>181</sup> W	21/2 <sup>+</sup>	182 ns	614	30	55	840	$\nu 9/2[624], \pi 5/2[402], \pi 7/2[404]$	$\nu 9/2[624]$	[27]
<sup>183</sup> W	19/2 <sup>-</sup>	13 ns	33	4.3	130	1087	$\nu 1/2[510], \nu 9/2[624], \nu 11/2[615]$	$\nu 7/2[503]$	[29]
<sup>181</sup> Re	21/2 <sup>-</sup>	250 ns	55	8.8	59	843	$\nu 7/2[514], \nu 9/2[624], \pi 5/2[402]$	$\pi 9/2[514]$	[30]
<sup>181</sup> Os	21/2 <sup>+</sup>	7 ns	848	13	464	932	$\nu 5/2[512], \nu 7/2[514], \nu 9/2[624]$	$\nu 9/2[624]$	[41]

<sup>a</sup>A negative sign indicates that the isomer is at lower energy than the collective state with which it mixes.

<sup>b</sup>Subsequent to Ref. [7], the <sup>173</sup>Ta isomer decay scheme was revised by Wood *et al.* [38].

<sup>c</sup>The <sup>179</sup>Ta isomer structure is strongly mixed [23], most likely with the  $\pi 5/2[402], \nu 7/2[514], \nu 9/2[624]$  configuration.

<sup>d</sup>Extrapolation of the collective band is necessary to obtain  $\Delta E$  for <sup>185</sup>Ta.

interaction matrix elements remain small, which is satisfied by  $|V| = 10$  eV in the <sup>164</sup>Er example, and  $|V|/\Delta E \leq 1.5\%$  in all cases.

It is worthwhile to remark that the smallest interactions obtained in this way are  $|V| = 0.46$  eV for the <sup>174</sup>Yb,  $K^\pi = 6^+$  isomer decay, where  $\Delta E = 992$  keV, and 1.4 eV for the <sup>177</sup>Hf,  $K^\pi = 23/2^+$  isomer decay, where  $\Delta E = -245$  keV (with the negative sign indicating that the isomer is at lower energy than the collective state with which it mixes). In comparison, Dracoulis *et al.* [15] found the smallest interactions to be in the range  $|V| = 10$ – $20$  eV, but that was considering chance near degeneracies, so the question again arises as to what criteria should be applied, and whether or not Eq. (7) remains valid.

A significant criterion for the validity of the two-state mixing analysis is that the relative  $B(M1)$  and  $B(E2)$  strengths from a given isomer should be the same as those in the rotational band to which the isomer decays [7,14,15,42,43]. However, as shown by Saitoh *et al.* [42,43], there are many examples where this criterion is violated, suggesting more complex mixing scenarios. In order to illustrate some specific aspects of the problem, the present work focuses on  $\Delta K = 6$ ,  $E2$  decays from 3- $qp$  isomers to 1- $qp$  rotational bands. The details are given in Table I. By restricting to only  $\Delta K = 6$  ( $\nu = 4$ ) transitions, any  $\Delta K$  dependence [15] is avoided. In addition, the mixing matrix element,  $|V|$ , can be considered to be an effective value, obtained from the two-state mixing equations.

### III. DEPENDENCE ON $E_K - E_R$

Before focusing on the systematic behavior of the interaction matrix elements, the corresponding reduced hindrances

( $f_\nu$  values) are presented. These are the quantities that are more usually compared [5,7]. For three- $qp$  isomer decays, the reduced hindrances were already shown [10] to be correlated with the isomer energy relative to a rigid-rotor energy, when the isomer structure is built on three  $qp$ 's of the same nucleon type, i.e., three protons or three neutrons. The full three- $qp$  data set, without the configuration restriction, but limited to  $\Delta K = 6$ ,  $E2$  transitions, is shown in Fig. 3, and the numerical values are in Table I. The quantity  $E_K - E_R$  is the difference between the isomer energy,  $E_K$ , and a rigid-rotor energy,  $E_R = aI(I + 1)$ , with  $I = K$  and  $a = \hbar^2/2J$ . Here, the moment of inertia is  $J = \frac{2}{5}mr^2(1 + \frac{1}{3}\beta_2)$ , where  $m$  is the mass and  $r$  is the radius. In practice, 85% of the full moment of inertia is used, taking into account the less-than-rigid moments of inertia of nuclei, and allowing better for a wide range of angular momenta [5]. The overall decrease in  $f_\nu$  with increasing  $E_K - E_R$  can be understood [5,11] as being due to the increasing level density as the isomer energy increases, leading to greater  $K$  mixing and hence lower  $f_\nu$  values.

The correlated behavior in Fig. 3 is reasonably clear, especially when it is noticed that the <sup>177</sup>Ta and especially the <sup>179</sup>Ta data points, at relatively low values of  $E_K - E_R$ , have chance near degeneracies, with  $\Delta E = +53$  and  $-29$  keV, respectively. Therefore, two-state mixing can explain their low  $f_\nu$  values (i.e., lower than might be expected from the overall trend of the data). However, there are other cases with similar or smaller  $\Delta E$ : <sup>171</sup>Tm ( $\Delta E = -11$  keV), <sup>183</sup>W (+33 keV), and <sup>181</sup>Re (+55 keV). This leads to the central issue of the present work: how the chance near degeneracies can be accounted for in a consistent manner.

In the light of the earlier discussion and the derivation of Eq. (7), it is here proposed that the mixing matrix element

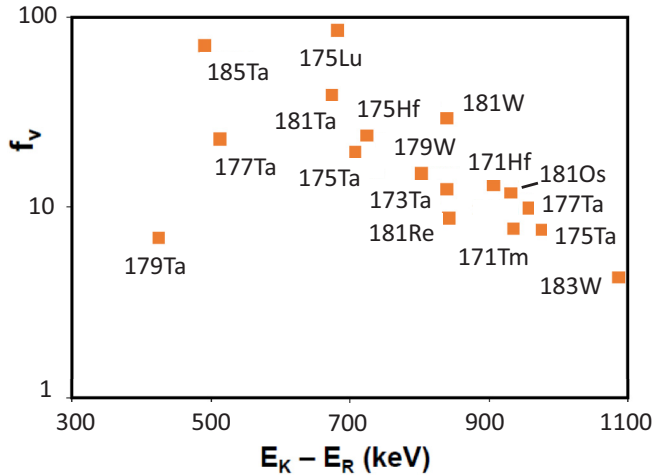


FIG. 3. Reduced hindrance,  $f_\nu$ , as a function of isomer energy relative to a rigid rotor,  $E_K - E_R$ , for  $\Delta K = 6$ ,  $E2$  decays from  $3\text{-}qp$  isomers in the  $Z \approx 70$  region. The subtracted rotor energy,  $E_R$ , has a moment of inertia that is 85% of the full rigid-body value (see text). Table I has the numerical values. Note that there are two data points for each of  $^{175}\text{Ta}$  and  $^{177}\text{Ta}$ . The statistical uncertainties are smaller than the data points.

$|V|$  itself is the appropriate variable that takes into account the closeness of the degeneracy. In order to compare with the  $f_\nu$  behavior of Fig. 3, it is necessary to evaluate the inverse of the mixing matrix element. Given that  $1/|V| \propto \sqrt{F_W}$ , and  $F_W = (f_\nu)^\nu$  with  $\nu = 4$ , it is evident that the  $1/|V|$  scale should, for the simplest comparison, have twice the number of decades as the  $f_\nu$  scale. This becomes clear in Fig. 4, where  $1/|V|$  is shown as a function of  $E_K - E_R$ .

At first sight, the scatter of the data in Fig. 4 looks greater than that in Fig. 3. The data points with closer near degeneracies have larger ordinate values compared with the overall behavior, as seen, for example, by the differences in the two figures for  $^{179}\text{Ta}$  with  $\Delta E = -29$  keV, and  $^{171}\text{Tm}$  with  $\Delta E = -11$  keV. In a real sense, the  $1/|V|$  evaluation removes the chance effect of near degeneracies. More careful inspection reveals some striking features, especially when the labels specifying the populated  $1\text{-}qp$  rotational-band configurations are included. Of the 17 data points, seven are for decays to a  $\pi 9/2[514]$  band. While one of these,  $^{179}\text{Ta}$ , is anomalous and will be discussed later in detail, the other six (inside the largest ellipse) are tightly correlated with  $E_K - E_R$ . A similar correlation persists with the five data points for decays to  $\nu i_{13/2}$  ( $7/2[633]$  and  $9/2[624]$ ) bands, and the two data points for decays to  $\pi 5/2[402]$  bands. The common behavior of decreasing  $1/|V|$  with increasing  $E_K - E_R$  supports the level-density effect referred to earlier. It can then be suggested that, compared to this trend, the larger  $1/|V|$  values for  $^{175}\text{Lu}$  and  $^{171}\text{Tm}$  ( $\pi 7/2[404]$ ) and  $^{183}\text{W}$  ( $\nu 7/2[503]$ ) are due to a smaller degree of Coriolis  $K$  mixing in these  $1\text{-}qp$  structures, where, with  $j = \Omega$ , the Coriolis matrix elements,  $H_c \propto \sqrt{j^2 - \Omega^2}$ , are close to zero [44].

The immediate problem appears to be that the  $^{175}\text{Ta}$  and  $^{177}\text{Ta}$  data points in Fig. 4, at  $E_K - E_R \approx 970$  keV, also

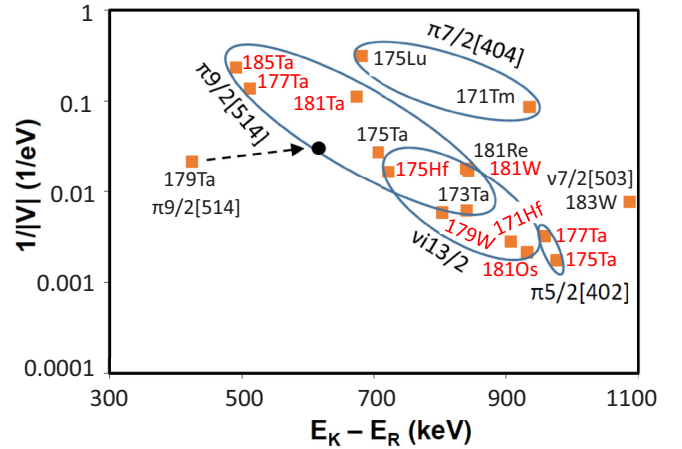


FIG. 4. Inverse interaction matrix element,  $1/|V|$ , as a function of energy relative to a rigid rotor,  $E_K - E_R$ , for  $\Delta K = 6$ ,  $E2$  decays from  $3\text{-}qp$  isomers in the  $Z \approx 70$  region. The Nilsson configurations of the populated  $1\text{-}qp$  bands are indicated. The subtracted rotor energy,  $E_R$ , has a moment of inertia that is 85% of the full rigid-body value. Table I has the numerical values. Note that the  $^{181}\text{W}$  and  $^{181}\text{Re}$  data points are overlapping. The filled circle is for  $^{179}\text{Ta}$ , replotted according to a three-level-mixing analysis (see text). The statistical uncertainties are smaller than the data points.

involve decay to a  $1\text{-}qp$  configuration,  $\pi 5/2[402]$ , with  $H_c \approx 0$ , and yet they have small  $1/|V|$  values. However, in addition to noting the large  $E_K - E_R$  values, these two data points can be partly understood in terms of Coriolis mixing in the isomers themselves. Their  $3\text{-}qp$  configurations include the  $h_{9/2}$ ,  $1/2[541]$  proton, which is well known for its strong Coriolis mixing effect [39]. None of the other  $3\text{-}qp$  configurations involves the  $1/2[541]$  proton.

Finally, the anomalous situation for the 1252 keV,  $K^\pi = 21/2^-$  isomer of  $^{179}\text{Ta}$  is discussed. While its  $1/|V|$  value (Fig. 4) is less deviant than its  $f_\nu$  value (Fig. 3), it still stands out as not following the trend of the other data. It can be considered to be a special case for two reasons: (i) there is a chance near degeneracy [7] at  $I^\pi = 21/2^-$ , with  $\Delta E = 29$  keV, and (ii) it has been proposed [23] that there is strong mixing with a second  $K^\pi = 21/2^-$  configuration. This latter feature is unique among the  $3\text{-}qp$  configurations of Figs. 3 and 4. Kondev *et al.* [23] studied the  $K^\pi = 21/2^-$  structure of  $^{179}\text{Ta}$  in detail and presented different mixing possibilities. Their favored interpretation is that there is  $\approx 50/50$  mixing between the two configurations given in Table I. The higher-energy  $K^\pi = 21/2^-$  state is suggested [23] to be that identified at 1628 keV. This implies that the maximum mixing matrix element would be  $|V| = \Delta E/2 = 188$  keV, which is similar to the 159 keV mixing between two  $K^\pi = 8^-$  states in the isotope  $^{178}\text{Hf}$  [45]. In terms of their configurations, the pair of states in  $^{178}\text{Hf}$  differ from that in  $^{179}\text{Ta}$  only by the removal of the spectator  $5/2[402]$  proton.

Such a large mixing strength of up to  $|V| = 188$  keV, between two states with the same  $K^\pi$ , is very different from that associated with the chance near degeneracy, with  $|V| = 47$  eV, between two states that differ in  $K$  by six units, and clearly



a three-state mixing calculation is required. While there are insufficient constraints to determine a unique solution, a simple possibility has been evaluated [46] with the maximum mixing strength (188 keV) between the two  $K^\pi = 21/2^-$  states, so that, before mixing, the unperturbed  $K^\pi = 21/2^-$  states are degenerate at 1440 keV. Equal but adjustable mixing strengths, between the  $I^\pi = 21/2^-$ ,  $\pi 9/2[514]$  band member and each of the two  $K^\pi = 21/2^-$  states, are chosen to give the observed  $K^\pi = 21/2^-$  isomer half-life. In this way,  $|V| = 33$  eV is obtained, compared to 47 eV in the two-state-mixing scenario. The new value is replotted as the filled circle in Fig. 4, with  $E_K - E_R = 612$  keV from the unperturbed  $K^\pi = 21/2^-$  energy of 1440 keV. The new value is seen to be consistent with the other data involving the population of the  $\pi 9/2[514]$  band. Therefore, it can be concluded that the anomalous character of  $^{179}\text{Ta}$  is due to its dual mixing components: strong mixing with another state of the same  $K^\pi$ , and weak mixing with a state of the same  $I^\pi$  but differing in  $K$  by six units.

Just as the proton-neutron  $K^\pi = 8^-$  mixing in  $^{178}\text{Hf}$  can be identified in its  $N = 106$  isotone  $^{179}\text{Ta}$ , so also it might be expected that the well-known proton-neutron  $K^\pi = 6^+$  mixing in  $^{176}\text{Hf}$  [7] might be reflected in its  $N = 104$  isotone  $^{177}\text{Ta}$ . Indeed, the  $K^\pi = 21/2^-$  isomer in  $^{177}\text{Ta}$  presents this possibility, which is discussed in detail by Dasgupta *et al.* [19]. Nevertheless, band-mixing calculations [19] suggest that, close to the  $K^\pi = 21/2^-$  bandhead, the structure is predominantly of three-proton character, as given in Table I. This, at least, is consistent with the corresponding  $1/|V|$  value following the general behavior seen in Fig. 4, i.e. it does not have the anomalous behavior shown by the  $K^\pi = 21/2^-$  isomer of  $^{179}\text{Ta}$ , where strong proton-neutron mixing is involved.

The stated criterion for the validity of the two-state mixing analysis is that the  $B(M1)/B(E2)$  ratio for the isomer decay should match that of the populated band or, equivalently, their  $g$  factors should be equal [7,14,15,42,43]. A simple test can be made with the rotational model expression [26],

$$\frac{|g_K - g_R|}{Q_0} = 0.933 \frac{E_{I \rightarrow I-1}}{\delta \sqrt{I^2 - 1}}, \quad (8)$$

where  $\delta$  is the quadrupole/dipole mixing ratio for the  $I \rightarrow I - 1$  transition and  $E_{I \rightarrow I-1}$  is the transition energy in MeV. The quantities  $g_K$  and  $g_R$  are the intrinsic and rotational  $g$  factors [26], respectively. As part of the present work,  $|g_K - g_R|$  was evaluated, where the data are available, for all the  $3-qp$  isomer decays illustrated in Fig. 4. For example, with  $Q_0 = 7$  b, for  $^{183}\text{W}$  [29] it is found that  $|g_K - g_R| = 0.96(3)$  for decays from the  $19/2^-$  isomer, and  $0.94(5)$  for decays

from the  $19/2^-$  member of the  $7/2[503]$  band. While this good agreement suggests the validity of the two-state mixing approach, the observation that in this case  $E_K - E_R$  is large and  $1/|V|$  is small indicates that other mixing processes are substantial. Indeed, the overall correlation with  $E_K - E_R$  in Fig. 4 suggests that level-density effects make a key contribution to the  $K$  mixing.

The  $|g_K - g_R|$  values also match, at least approximately, for  $^{171}\text{Tm}$ ,  $^{175}\text{Lu}$ ,  $^{173}\text{Ta}$ ,  $^{175}\text{Ta}$ ,  $^{179}\text{Ta}$ , and  $^{181}\text{Re}$  (with black lettering in Fig. 4), while the other ten cases (with red lettering) do not, and it is hard to interpret these differences. We suggest, therefore, that the comparison of  $B(M1)/B(E2)$  values is of limited practical value. Nevertheless, it is appropriate to refer to the mixing matrix elements of Table I and Fig. 4 as effective values.

By focusing in this work on  $E2$ ,  $\Delta K = 6$  ( $\nu = 4$ ) transitions, the  $\Delta K$  dependence has been avoided. While  $\Delta K$  is explicitly taken into account in the formulation of the reduced hindrance,  $f_\nu = (F_W)^{1/\nu}$ , which has no units, the mixing matrix element,  $|V|$ , has energy units, which need to be properly accounted for if transitions with different  $\Delta K$  are to be compared. Nevertheless, extension of the work of Dracoulis *et al.* [15] to study the  $\Delta K$  dependence of  $|V|$  is planned for the future. Also, it is appropriate to investigate the role of higher  $qp$  numbers. A preliminary analysis of this type, limited to  $\Delta K = 6$  transitions, has been undertaken, but the shortage of data and the increased complexity of the configurations make it difficult to come to conclusions about the general behavior.

#### IV. CONCLUSION

In summary, for  $E2$ ,  $K$ -isomer decays, a simple formula has been established relating the Weisskopf hindrance factor,  $F_W$ , to the effective mixing matrix element,  $|V|$ , between the isomer itself and the state of the same  $I^\pi$  in the populated band. In principle, the  $|V|$  formulation removes dependence on the chance effect of near degeneracies. Decays with  $\Delta K = 6$  from  $3-qp$  isomers in the  $Z \approx 70$  region have been analyzed in detail, revealing new evidence for significant configuration dependence, with regard to both the populated band as well as the isomer itself. Of the 17 data points, just one, that for the  $^{179}\text{Ta}$ ,  $K^\pi = 21/2^-$  isomer, appears to be inconsistent with the general behavior, which is interpreted as being due to strong  $\Delta K = 0$  configuration mixing.

#### ACKNOWLEDGMENTS

This work is supported by Grant No. ST/P005314/1 from the UK Science and Technology Facilities Council.

- [1] P. M. Walker and G. D. Dracoulis, *Nature (London)* **399**, 35 (1999).
- [2] P. M. Walker and J. J. Carroll, *Physics Today* **58**(6), 39 (2005).
- [3] A. K. Jain, B. Maheshwari, S. Garg, M. Patial, and B. Singh, *Nucl. Data Sheets* **128**, 1 (2015).
- [4] P. M. Walker and Zs. Podolyák, *Phys. Scr.* **95**, 044004 (2020).

- [5] G. D. Dracoulis, P. M. Walker, and F. G. Kondev, *Rep. Prog. Phys.* **79**, 076301 (2016).
- [6] F. G. Kondev, M. Wang, W. J. Huang, S. Naimi, and G. Audi, *Chin. Phys. C* **45**, 030001 (2021).
- [7] F. G. Kondev, G. D. Dracoulis, and T. Kibédi, *At. Data Nucl. Data Tables* **103–104**, 50 (2015).
- [8] G. D. Dracoulis *et al.*, *Phys. Rev. C* **79**, 061303(R) (2009).

- [9] P. M. Walker, *J. Phys. G: Nucl. Phys.* **16**, L233 (1990).
- [10] P. M. Walker, S. Lalkovski, and P. D. Stevenson, *Phys. Rev. C* **81**, 041304(R) (2010).
- [11] P. M. Walker *et al.*, *Phys. Lett. B* **408**, 42 (1997).
- [12] P. M. Walker, *Phys. Scr.* **92**, 054001 (2017).
- [13] R. F. Casten, *Nuclear Structure from a Simple Perspective* (Oxford University Press, Oxford, 2000).
- [14] P. M. Walker *et al.*, *Phys. Rev. C* **79**, 044321 (2009).
- [15] G. D. Dracoulis *et al.*, *Phys. Rev. Lett.* **97**, 122501 (2006).
- [16] A. Bohr and B. R. Mottelson, *Nuclear Structure* (World Scientific, Singapore, 1998), Vol. II.
- [17] P. Campbell, I. D. Moore, and M. R. Pearson, *Prog. Part. Nucl. Phys.* **86**, 127 (2016).
- [18] P. Möller, A. J. Sierk, T. Ichikawa, and H. Sagawa, *At. Data Nucl. Data Tables* **109–110**, 1 (2016).
- [19] M. Dasgupta, G. D. Dracoulis, P. M. Walker, A. P. Byrne, T. Kibédi, F. G. Kondev, G. J. Lane, and P. H. Regan, *Phys. Rev. C* **61**, 044321 (2000).
- [20] R. O. Hughes *et al.*, *Phys. Rev. C* **86**, 054314 (2012).
- [21] G. D. Dracoulis *et al.*, *Phys. Rev. C* **71**, 044326 (2005).
- [22] T. R. McGoram, G. D. Dracoulis, T. Kibédi, A. P. Byrne, R. A. Bark, A. M. Baxter, and S. M. Mullins, *Phys. Rev. C* **62**, 031303(R) (2000).
- [23] F. G. Kondev, G. D. Dracoulis, A. P. Byrne, T. Kibédi, and S. Bayer, *Nucl. Phys. A* **617**, 91 (1997).
- [24] F. G. Kondev *et al.*, *Eur. Phys. J. A* **22**, 23 (2004).
- [25] T. Shizuma *et al.*, *Nucl. Phys. A* **626**, 760 (1997).
- [26] P. M. Walker, G. D. Dracoulis, A. P. Byrne, T. Kibédi, B. Fabricius, A. E. Stuchbery, and N. Rowley, *Nucl. Phys. A* **568**, 397 (1994).
- [27] K. C. Yeung, Ph.D. Thesis, University of Surrey, 1993.
- [28] P. H. Regan, P. M. Walker, G. D. Dracoulis, S. S. Anderssen, A. P. Byrne, P. M. Davidson, T. Kibédi, G. J. Lane, A. E. Stuchbery, and K. C. Yeung, *Nucl. Phys. A* **567**, 414 (1994).
- [29] T. R. Saitoh, N. Saitoh-Hashimoto, G. Sletten, R. A. Bark, M. Bergström, P. H. Regan, S. Törmänen, P. G. Varmette, P. M. Walker, and C. Wheldon, *Nucl. Phys. A* **669**, 381 (2000).
- [30] C. J. Pearson, P. M. Walker, C. S. Purry, G. D. Dracoulis, S. Bayer, A. P. Byrne, T. Kibédi, and F. G. Kondev, *Nucl. Phys. A* **674**, 301 (2000).
- [31] F. G. Kondev, M. A. Riley, D. J. Hartley, R. W. Laird, T. B. Brown, M. Lively, K. W. Kemper, J. Pfohl, S. L. Tabor, and R. K. Sheline, *Phys. Rev. C* **59**, 575(R) (1999).
- [32] O. Möller *et al.*, *Phys. Rev. C* **72**, 034306 (2005).
- [33] T. Shizuma, P. D. Stevenson, P. M. Walker, Y. Toh, T. Hayakawa, M. Oshima, K. Furuno, and T. Komatsubara, *Phys. Rev. C* **65**, 064310 (2002).
- [34] T. P. D. Swan, P. M. Walker, Zs. Podolyák, M. W. Reed, G. D. Dracoulis, G. J. Lane, T. Kibédi, and M. L. Smith, *Phys. Rev. C* **86**, 044307 (2012).
- [35] C. Wheldon *et al.*, *Phys. Lett. B* **425**, 239 (1998).
- [36] G. D. Dracoulis, P. M. Walker, and K. F. Lee, *J. Phys. G: Nucl. Phys.* **5**, L19 (1979).
- [37] G. D. Dracoulis and P. M. Walker, *Nucl. Phys. A* **342**, 335 (1980).
- [38] R. T. Wood *et al.*, *Phys. Rev. C* **95**, 054308 (2017).
- [39] F. G. Kondev, G. D. Dracoulis, A. P. Byrne, M. Dasgupta, T. Kibédi, and G. J. Lane, *Nucl. Phys. A* **601**, 195 (1996).
- [40] G. J. Lane *et al.*, *Phys. Rev. C* **80**, 024321 (2009).
- [41] D. M. Cullen *et al.*, *Nucl. Phys. A* **728**, 287 (2003).
- [42] T. R. Saitoh *et al.*, *Nucl. Phys. A* **660**, 121 (1999).
- [43] T. R. Saitoh, N. Saitoh-Hashimoto, G. Sletten, R. A. Bark, G. B. Hagemann, and B. Herskind, *Phys. Scr. T* **88**, 67 (2000).
- [44] F. S. Stephens, *Rev. Mod. Phys.* **47**, 43 (1975).
- [45] M. B. Smith, P. M. Walker, G. C. Ball, J. J. Carroll, P. E. Garrett, G. Hackman, R. Propri, F. Sarazin, and H. C. Scraggs, *Phys. Rev. C* **68**, 031302(R) (2003).
- [46] See Supplemental Material at <http://link.aps.org/supplemental/10.1103/PhysRevC.103.064305> for the three-level-mixing Maple worksheet.